Identification of a buried β-strand as a novel disease-related motif in the human polysialyltransferases

Received for publication, July 16, 2023, and in revised form, November 26, 2023 Published, Papers in Press, December 14, 2023,
https://doi.org/10.1016/j.jbc.2023.105564

Rina Hatanaka[1,2,3], **Masaya Hane**[1,2,3], **Kaito Hayakawa**[1,2,3], **Sayo Morishita**[1,2,3], **Shiho Ohno**[4], **Yoshiki Yamaguchi**[4], **Di Wu**[1,2,3], **Ken Kitajima**[1,2,3], and **Chihiro Sato**[1,2,3,*]

From the [1]*Integrated Glyco-BioMedical Research Center (iGMED), Institute for Glyco-core Research (iGCORE),* [2]*Bioscience and Biotechnology Center, and* [3]*Graduate School of Bioagricultural Sciences, Nagoya University, Nagoya, Japan;* [4]*Division of Structural Biology, Institute of Molecular Biomembrane and Glycobiology, Tohoku Medical and Pharmaceutical University, Sendai, Japan*

Reviewed by members of the JBC Editorial Board. Edited by Robert Haltiwanger

The polysialyltransferases ST8SIA2 and ST8SIA4 and their product, polysialic acid (polySia), are known to be related to cancers and mental disorders. ST8SIA2 and ST8SIA4 have conserved amino acid (AA) sequence motifs essential for the synthesis of the polySia structures on the neural cell adhesion molecule. To search for a new motif in the polysialyltransferases, we adopted the *in silico* Individual Meta Random Forest program that can predict disease-related AA substitutions. The Individual Meta Random Forest program predicted a new eight-amino-acids sequence motif consisting of highly pathogenic AA residues, thus designated as the pathogenic (P) motif. A series of alanine point mutation experiments in the pathogenic motif (P motif) showed that most P motif mutants lost the polysialylation activity without changing the proper enzyme expression levels or localization in the Golgi. In addition, we evaluated the enzyme stability of the P motif mutants using newly established calculations of mutation energy, demonstrating that the subtle change of the conformational energy regulates the activity. In the AlphaFold2 model, we found that the P motif was a buried β-strand underneath the known surface motifs unique to ST8SIA2 and ST8SIA4. Taken together, the P motif is a novel buried β-strand that regulates the full activity of polysialyltransferases from the inside of the molecule.

Sialic acid (Sia) forms glycan epitopes essential for many biological functions including embryogenesis, fertilization, development, and the immune and nervous systems (1). The expression of Sia-glycan epitopes is highly regulated by synthetic enzymes known as sialyltransferases (STs), and the impairment of Sia expression has been reported to be related to diseases such as infection, cancer, and mental disorders (2). Among Sia epitopes, polysialic acid (polySia), a polymer of Sia, is a well-known development- and disease-related epitope (3). PolySias are enriched in the embryonic brain and mostly disappear in the adult brain. However, in restricted brain areas, such as the olfactory bulb system and hippocampus, where neural remodeling is active, the polySia expression continues even in adult brains (4). The functions of polySia are demonstrated to display a repulsive field owing to its hydration effect (5) and an attractive field (6–8) by capturing neurotrophic and growth factors in the polySia chains to regulate the concentration of the molecules outside the cells. Through these features, polySia has been shown to be involved in cell-to-cell interactions, cell migration, axonal guidance, fasciculation, myelination, synapse formation, and the functional plasticity of the nervous system (8). The impairment of polySia's expression and functions leads to diseases such as cancer and mental disorders (3).

STs are responsible for the synthesis of Sia epitopes on glycoconjugates, transferring Sia residue from the donor substrate cytidine 5′-monophospho-sialic acid (CMP-Sia) to the glycan residues in glycoproteins and glycolipids. In humans, 20 kinds of STs have been cloned and grouped into four families, ST3GAL, ST6GAL, ST6GALNAC, and ST8SIA, based on their linkage and acceptor specificities (9). ST8SIAs are α2,8-sialyltransferases that transfer Sia to Sia residue *via* the α2,8-linkage, synthesizing polymerized structures with degree of polymerization (DP) 2 to less than 400 (10). ST8SIA1 (GD3/GT3 synthetase, SAT-II/III, SIAT8A) (11) and ST8SIA5 (SAT-V, SIAT8E) (12) are involved in the synthesis of b- and c-series gangliosides. ST8SIA3 (SIAT8C), whose X-ray crystal structure has been recently solved (13), can synthesize oligosialic acid on glycoproteins, glycolipids, and free oligosaccharides (14). ST8SIA6 (SIAT8F) is an oligosialyltransferase that transfers Sia to Sia residue on the *O*-glycans of proteins (15). ST8SIA2 (STX, SIAT8B) (16, 17) and ST8SIA4 (PST-1, SIAT8E) (18) are polysialyltransferases (polySTs) characterized by their ability to synthesize polySia structures. STs are type II transmembrane proteins, and most of them are localized in the Golgi apparatus except ST8SIA6 (19). These enzymes are modified for correct folding by post-translational modifications such as glycosylation, S-S formation, and oligomerization. Occasionally, these modifications are essential for the enzyme activity. Notably, the domain structures of these enzymes are highly conserved: they consist of a very short cytoplasmic region, a transmembrane region, a stem region,

* For correspondence: Chihiro Sato, chi@agr.nagoya-u.ac.jp.

and a catalytic domain in the intraluminal region. The catalytic region consists of sialyl motifs L, S, III, and VS, which are common in α2,3-, α2,6-, and α2,8-sialyltransferases of the CAZy GT29 family (2). Although the whole sequence homology was low among STs, these sialyl motifs are highly homologous among them and share the common functional importance: sialyl motif L serves as a binding site for the donor substrate (CMP-Sia); sialyl motif S serves as a binding site for both the donor and acceptor substrates; sialyl motif III is located between sialyl motifs S and VS and is involved in the catalytic activity; and the histidine residue of the sialyl motif VS is involved in the catalytic activity. More Recently, the polySTs, ST8SIA2 and ST8SIA4, were shown to have two additional motifs specific to these proteins: a polybasic region (PBR) and a polysialyltransferase domain (PSTD) which exist next to sialyl motif L and sialyl motif S, respectively (20). These two regions are highly conserved between ST8SIA2 and ST8SIA4 and are shown to be essential for the polysialylation on particular two *N*-linked glycans in the Ig5 domain of the neural cell adhesion molecule (NCAM). Especially, PBR binds to the acidic patch of the first FN_{III} domain of NCAM, and through this binding, ST8SIA2 and ST8SIA4 can specifically synthesize polySia on NCAM. Although it has been shown that the polySTs can also synthesize polySia onto glycoproteins other than NCAM (21–24), this new motif can consistently explain the fact that the major acceptor of polySTs in nature is NCAM. For example, the 1500-fold effective polysialylation was achieved on NCAM compared to other typical *N*-glycans on bi-, tri-, and tetra-antennary glycans on model glycoproteins (25) and 95% of polysialylation disappeared (26) in NCAM-knock out (KO) mice (27).

Taken together, the finding of new motifs in polySTs has greatly advanced our knowledge on the structure-function relationship of the enzymes. Recently, a random forest-based program (Individual Meta Random Forest, InMeRF) which is a new program to find a disease-related motif has been developed (28) and available on the website together with a training database. In this study, to gain a new insight into the motif structure related to human diseases, we adopted InMeRF to find a new disease-related motif and confirmed its significance based on biochemical and cell biological analyses.

Results

Finding a new motif

The amino acid (AA) sequences of ST8SIA2 and ST8SIA4, which are polySTs synthesizing polySia structures, are aligned (Fig. 1*A*). They exhibit 56.2% homology and contain several known motifs or regions, including the potential *N*-glycosylation sites. Sialyl motifs L, S, VS, and III are common motifs among all STs (Fig. S1). PolySTs have two additional common regions that are not conserved in other STs, the PBR and the PSTD (20, 29).

To search for a new potential sialyl motif that is important for the polyST functions, the InMeRF calculation program which can predict pathogenic AA residues was adopted for ST8SIA2 and ST8SIA4 (Fig. 1*B*). All the sialyl motifs L, S, VS, and III were found to contain pathogenic AA residues: % pathogenicity values were 66.7% (ST8SIA2) and 75.6% (ST8SIA4) for L; 78.2% (ST8SIA2) and 82.6% (ST8SIA4) for S; 66.7% (ST8SIA2) and 66.7% (ST8SIA4) for VS; and 100% (ST8SIA2) and 100% (ST8SIA4) for III. In addition, the polyST-specific regions PBR and PSTD also contained pathogenic AA residues, although the pathogenic residues were less frequently detected in PSTD than in PBR: % pathogenicity values were 54.3% (ST8SIA2) and 34.3% (ST8SIA4) for PBR and 42.9% (ST8SIA2) and 21.9% (ST8SIA4) for PSTD. These data showed that known conserved motifs and regions are pathogenic on the InMeRF, suggesting that impaired alterations in these regions may cause some diseases. Notably, a new cluster of pathogenic AA residues was found between sialyl motif L and PSTD (Fig. 1, *B* and *C*). This motif consisted of eight AA residues (SILWIPAF for ST8SIA2; SVLWIPAF for ST8SIA4) and was designated as pathogenic motif (P motif), because it showed 100% pathogenicity on the InMeRF.

The expression and enzyme activity of P motif mutants of polySTs

To investigate if the P motif was involved in the enzyme activities of ST8SIA2 and ST8SIA4, a series of expression plasmids encoding point-mutated polySTs in which each residue in the P motif was altered to alanine residue were prepared, and Neuro2A cells were transfected with each of the plasmid, followed by the analysis of the enzyme and polySia-NCAM expression. First, the enzyme expression level of each mutant, as evaluated by Western blotting using the anti-His antibody after Peptide-*N*-Glycosidase F (PNGaseF) treatment, was roughly the same as that of the wildtype (WT), except P241A of ST8SIA2 which was not expressed at all (Figs. 2*A* and 3*A*). The differences in the size of the WT and P motif mutants of ST8SIA2 and ST8SIA4 before and after PNGase F treatment were attributable to the presence of two *N*-glycans at N234 and N219. The weak staining before PNGaseF treatment observed for the WT, S236A, F243A, and R246A of ST8SIA2 and the WT, S221A, P226A, V230A, and K231A of ST8SIA4 was probably due to the presence of autopolysialylation on the enzymes, because it became strong one after de-*N*-glycosylation by PNGaseF. Then, the polySia expression level was also analyzed using the anti-oligo/polySia antibody 12E3 and the anti-polySia antibody 735. Prominently, the P motif mutants I237A to M244A for ST8SIA2 and V223A to F228A for ST8SIA4 showed extremely low polySia levels compared to the WT (Figs. 2, *B* and *C* and 3, *B* and *C*). To exclude the possibility that the low polySia level was due to the mislocalization of the enzymes, immunocytochemistry was performed using the anti-V5 antibody (Figs. 4 and 5). The anti-TGN antibody was also used for trans-Golgi staining, because polySTs are usually localized in the trans-Golgi or trans-Golgi networks. The results showed that the P motif mutants and WT enzymes were all localized to the TGN, except the unexpressed P241A of ST8SIA2 (see above). Taken together, the P motif mutants are suggested to significantly affect the

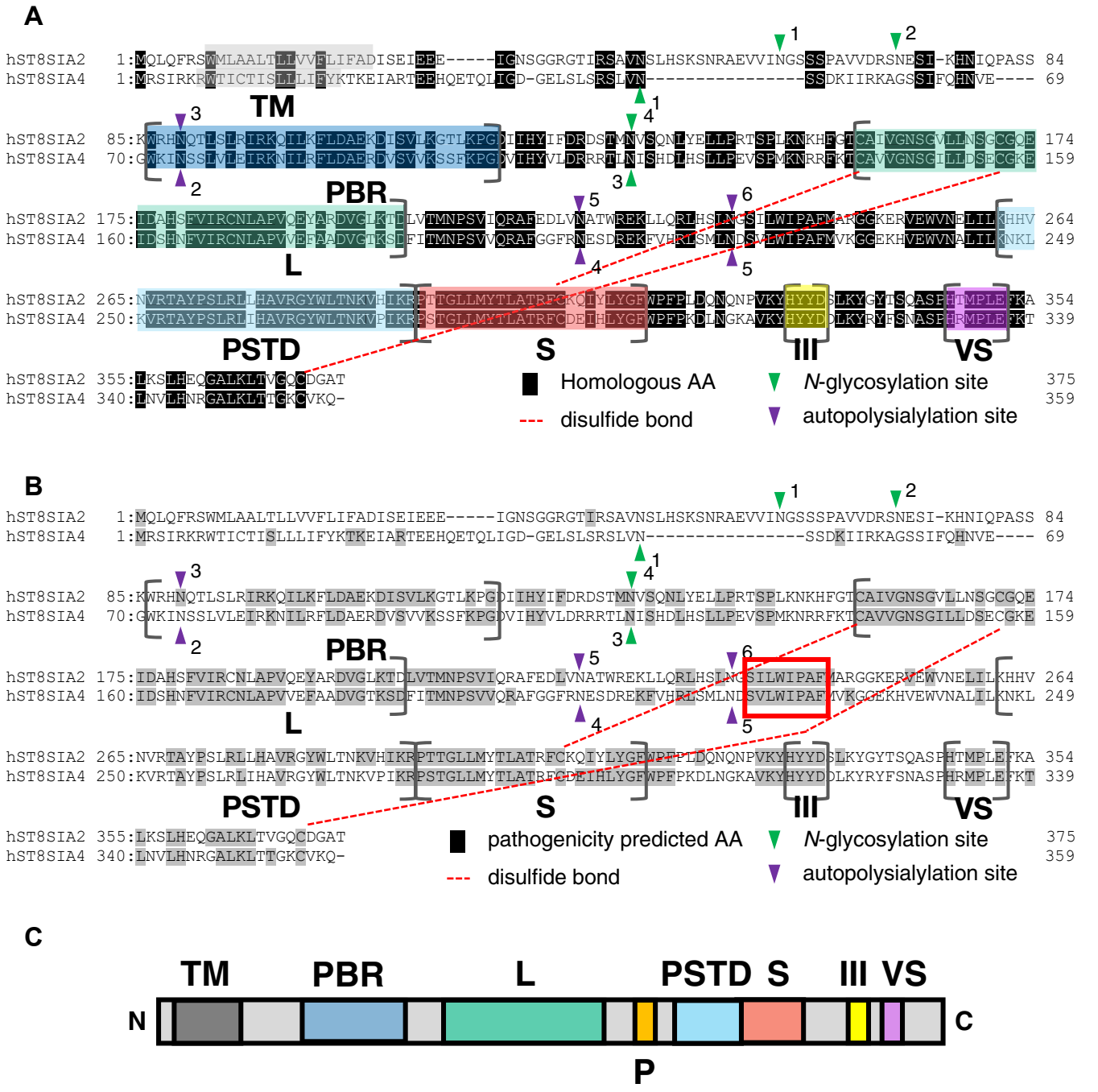

Figure 1. Comparison of the amino acid sequences of ST8SIA2 and ST8SIA4. *A*, homology alignment of ST8SIA2 and ST8SIA4. *Black* indicates the same amino acid. *B*, pathogenicity predictions for ST8SIA2 and ST8SIA4 based on the InMeRF program. L, S, III, and VS stand for the sialyl motifs long (L), short (S), III, and very short (VS), respectively. *Gray* is the pathogenic amino acid predicted by InMeRF (>0%), and *red box* is the region that was predicted and assigned as a pathogenic motif. *C*, schematic diagram of the sialyl motifs and PBR and PSTD regions on the polySTs. AA, amino acid; InMeRF, Individual Meta Random Forest; PBR, the polybasic region; polySTs, polysialyltransferases; PSTD, polysialyltransferase domain.

enzyme activity without changing in proper folding and normal localization in the Golgi.

Energy calculation of mutations for polySTs

To evaluate the effects of each of the alanine mutations in the P motif on conformational stability of the polySTs, we calculated the mutation energy which corresponds to the difference in Gibbs free energy between WT and the mutant. The results are shown in Figure 6. The alanine mutants exhibited −0.3 to 5.8 kcal/mol for ST8SIA2 and −1.2 to 5.9 kcal/mol for ST8SIA4 (Fig. 6, Left panel). I237A to M244A for ST8SIA2 and V222A to F228A for ST8SIA4 showed relatively higher mutation energy. All the mutants showed dramatically reduced activity (Figs. 2 and 3). For the AA residues within the P motif, not only alanine mutation but also other AA mutations showed similar changes in the mutation energy (Fig. 6, right panel). However, the expression of the enzymes, except for

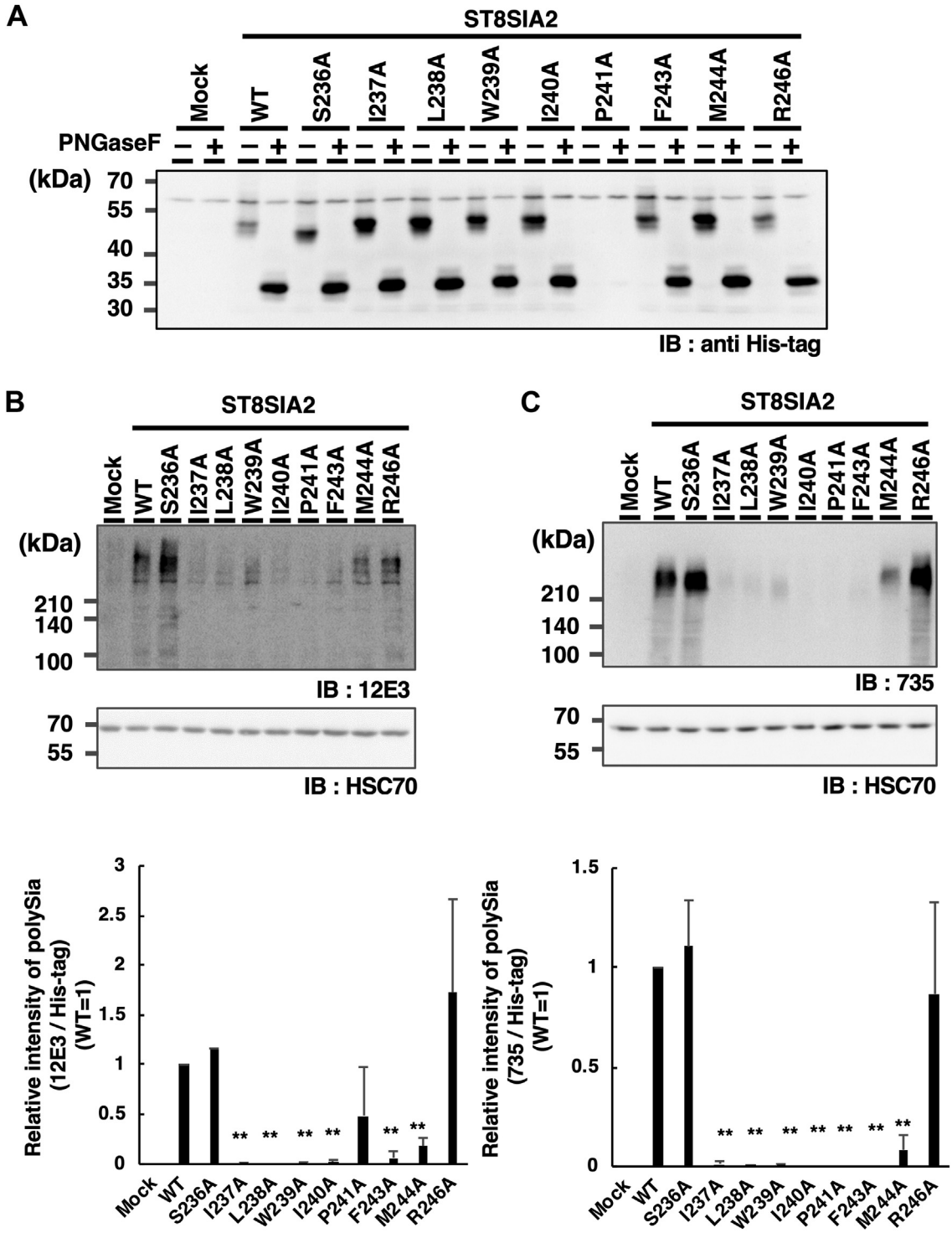

Figure 2. Effects of alanine point mutations in the P motif (236–246) of ST8SIA2 on the enzyme and polySia expression. *A*, the expression of the ST8SIA2 protein. WT or the P motif mutants of ST8SIA2 from each transient cell homogenate was analyzed by anti-His-tag antibody. For quantification, PNGaseF treatment was performed (PNGase+). *B*, the expression of polySia evaluated by 12E3. The same cell homogenates were analyzed using the anti-oligo/polySia antibody 12E3. *C*, the expression of polySia evaluated by 735. The same cell homogenates were analyzed by the anti-polySia antibody 735. Anti-HSC70 blot was the loading control. $^{**}p < 0.01$. PNGaseF, Peptide-*N*-Glycosidase F; polySia, polysialic acid.

P241A of ST8SIA2 (Figs. 2 and 3*B*), and their localizations (Figs. 4 and 5) did not change, indicating that the activity of the enzymes was influenced by a subtle change (1.0–5.9 kcal/mol) in mutation energy. The mutation energy, roughly 0.7 kcal of V230A of ST8SIA4, did not change its activity, but 0.9 kcal of M229A of ST8SIA4 showed half the activity (Fig. 3*B*). In the case of M244A of ST8SIA2, the mutation energy change was 1.3 kcal/mol, but the activity dramatically decreased (Fig. 2*B*), indicating that the change of 1 kcal/mol in the essential region led to a drastic change in enzymatic activity.

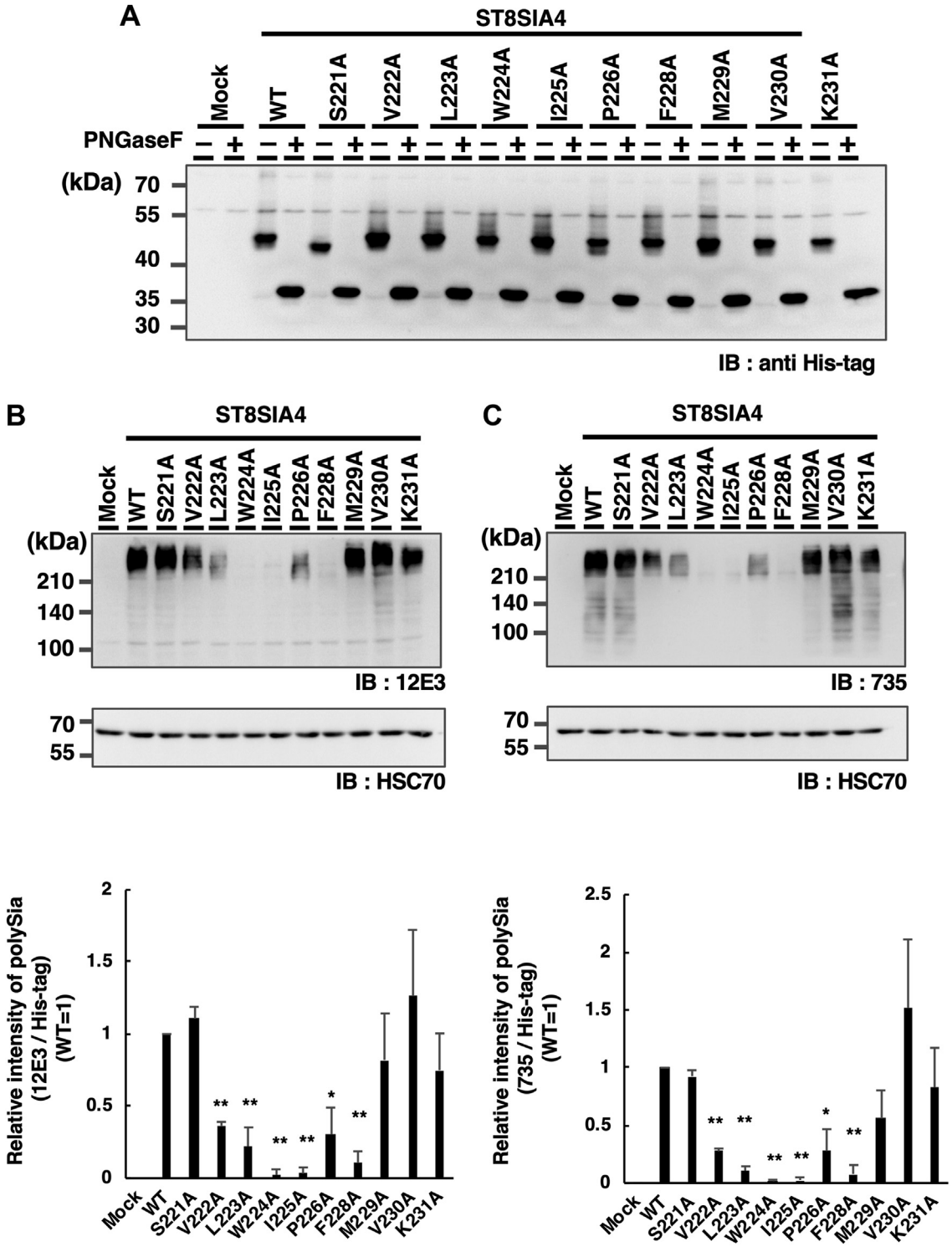

Figure 3. Effects of alanine point mutations in the P motif (221–231) of ST8SIA4 on the enzyme and polySia expression. *A*, the expression of the ST8SIA4 protein. WT or the P motif mutants of ST8SIA2 from each transient cell homogenate was analyzed by anti-His-tag antibody. For quantification, PNGaseF treatment was performed (PNGase+). *B*, the expression of polySia evaluated by 12E3. The same cell homogenates were analyzed by the anti-oligo/polySia antibody 12E3. *C*, the expression of polySia evaluated by 735. The same cell homogenates were analyzed by the anti-polySia antibody 735. Anti-HSC70 blot was the loading control. $^{**}p < 0.01$, $^{*}p < 0.05$. PNGaseF, Peptide-*N*-Glycosidase F; polySia, polysialic acid.

Modeling the structures of polySTs

To gain insight into the new motif or P motif, we modeled the structures of ST8SIA2 and ST8SIA4 using AlphaFold2 (30, 31). The ribbon and space-filling models are shown in Figure 7, in which the P motif is colored in orange. Other side views of the space filling models are shown in Fig. S4. The P motif was located on the sixth β-strand, which was the last part of the sequential β-strands ranging from the sialyl motif L (third and

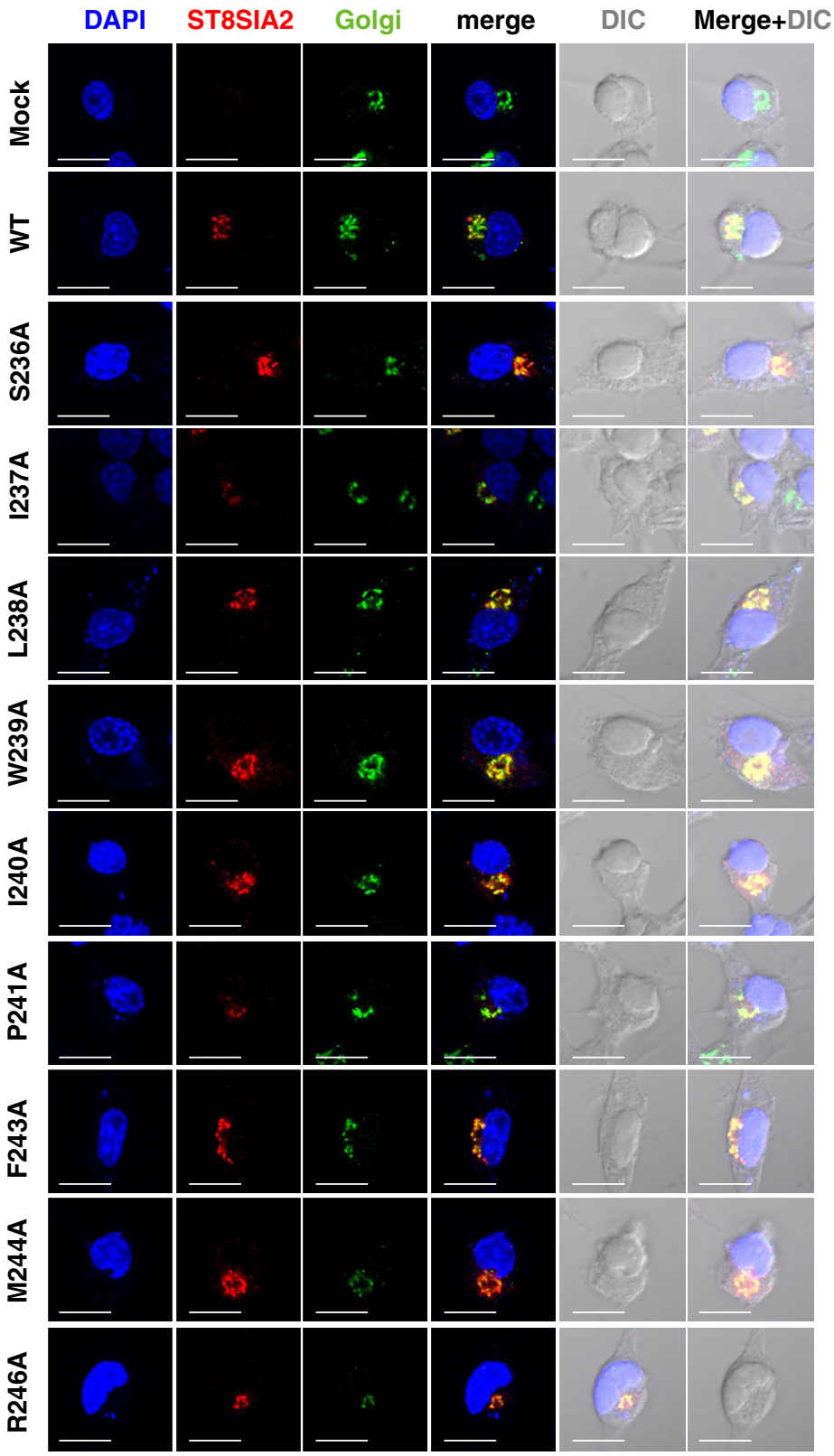

Figure 4. Immunolocalization of ST8SIA2. The cells transfected with plasmids coding ST8SIA2 or its P motif mutants were analyzed by staining with the anti-V5 antibody: ST8SIA2 (*red*) and anti-TGN46 antibody (*green*, Golgi). DAPI (*blue*) staining showed the nucleus. Scale bars, 10 μm.

fourth β-strands) down to the P motif through the region right after the sialyl motif L (fifth β-strand). In the space-filling model, the P motif was found to reside inside the molecule and underneath the surface layer formed by the sialyl motif L and PSTD. Thus, the P motif is a buried β-strand that is situated close to the PSTD which is essential region for polysialylation.

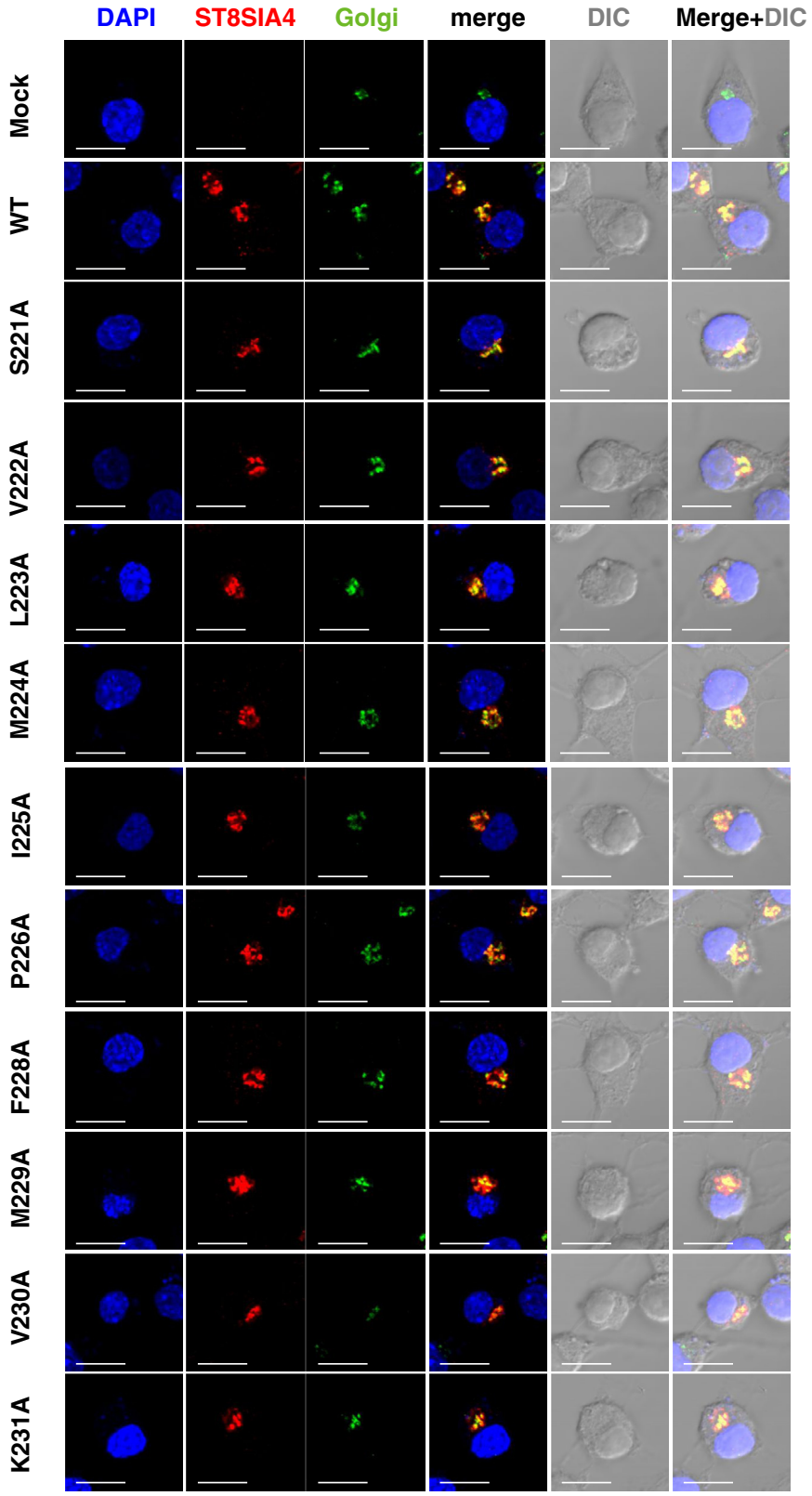

Figure 5. Immunolocalization of ST8SIA4. The cells transfected with plasmids coding ST8SIA4 or its P motif mutants were analyzed by staining with the anti-V5 antibody: ST8SIA4 (*red*) and anti-TGN46 antibody (*green*, Golgi). DAPI (*blue*) staining showed the nucleus. Scale bars, 10 μm.

Discussion

To date, several common structural motifs important for the ST activity have been demonstrated to be involved in the donor substrate CMP-Sia binding and/or the acceptor–substrate recognition (2). These motifs were first proposed based on the conserved AA sequences among STs and then

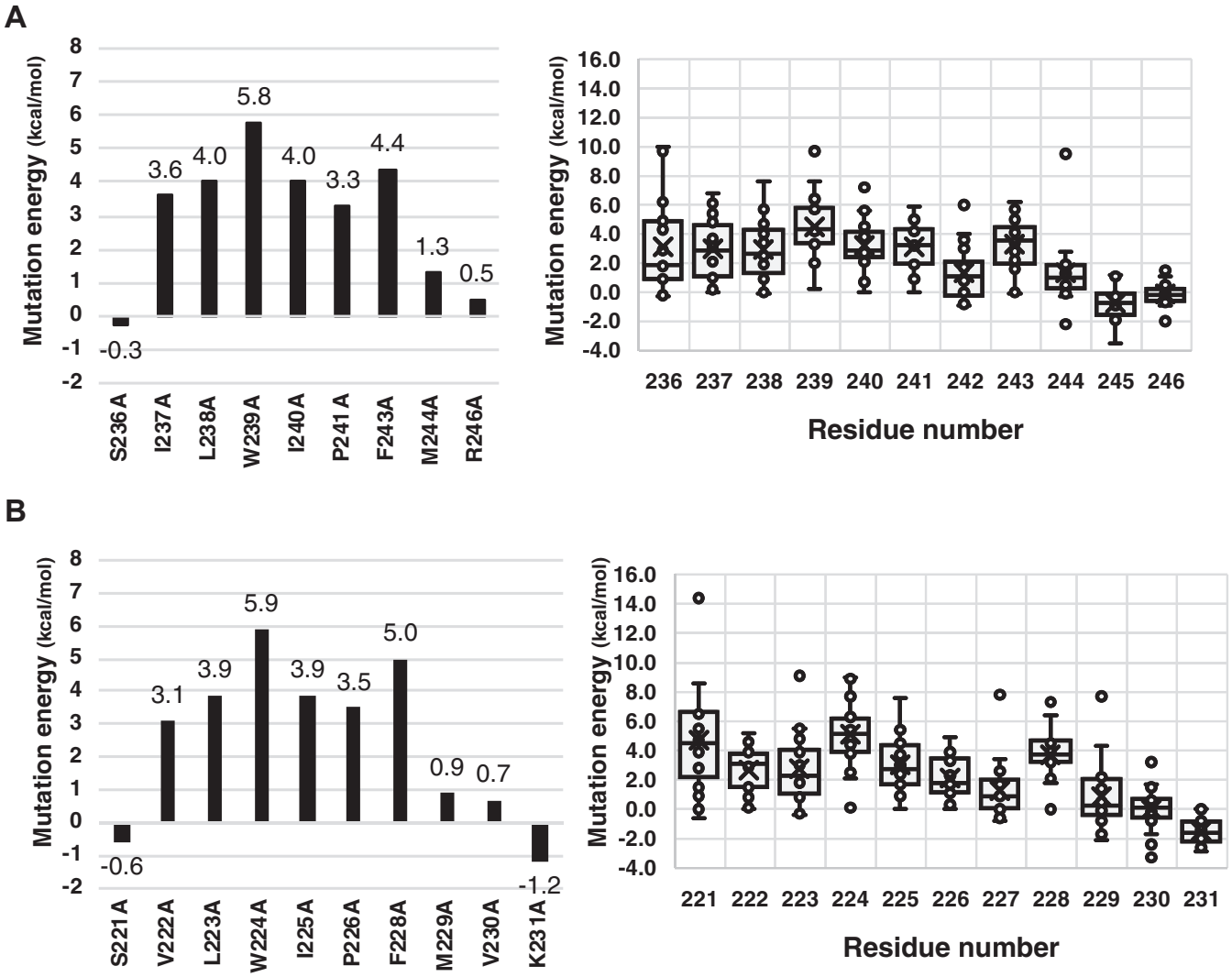

Figure 6. Mutation energy for ST8SIA2 and ST8SIA4. *A* and *B*, mutation energies were calculated for ST8SIA2 (*A*) and ST8SIA4 (*B*). *Left panel*, Ala mutations; *Right panel*, Mutations to all possible amino acids. Each plot in the graph corresponds to each of the 20 amino acids, though unspecified here.

biochemically characterized for the role in the enzyme reaction by their point mutations and subsequent evaluation of the catalytic activity. For example, previous reports showed that the sialyl motifs L, S, III, and VS (Fig. 1*A*) are essential for the ST activity: the sialyl motif L is involved in donor-substrate binding (CMP-Sia) (32, 33); the sialyl motif S is involved in both donor and acceptor substrates recognition (33); and the histidine (H) residues in the sialyl motifs III and VS are crucial for the activity. Thus, finding of conserved sialyl motifs in the STs would often lead us to understanding their roles in the STs functioning. To search for new regions or AA residues essential for the enzyme activity of polySTs, in this study, we first adopted the InMeRF program (28). This program has been developed to predict if single nucleotide mutations, which may cause changes in the corresponding AA residues, have the potential to damage the protein functions that may cause a sort of pathogenicity. It can thus provide information on the common domains or fundamental regions in the STs whose mutations may change enzymatic activities, acceptor binding, or complex formations, possibly leading to diseases. All human STs cloned to date were analyzed by this program, and all the highly conserved AA residues in these sialyl motifs L, S, III, and VS were predicted to be pathogenic with high count rates (Fig. S1). In addition, a number of AA residues in the polySTs-specific motifs PSTD and PBR, which are essential for the polysialylation of two particular *N*-glycans of NCAM, are also predicted to be pathogenic in ST8SIA2 and ST8SIA4, but not in most other STs (Fig. 1*B*). These results suggest that the InMeRF prediction program is effective for finding pathogenic regions in the STs, including polySTs.

Interestingly, in addition to the known sialyl motifs, a new highly pathogenic region is found between the sialyl motif L and PSTD in ST8SIA2 and ST8SIA4 (Figs. 1*B* and S1) and designated P motif. This eight-AA-sequence including the sixth β-strand (Fig. S1). The significance of this motif in the enzyme activity of ST8SIA2 and ST8SIA4 was demonstrated by the point mutation experiments as well as the localization studies (Figs. 2–5) and mutation energy calculation (Fig. 6).

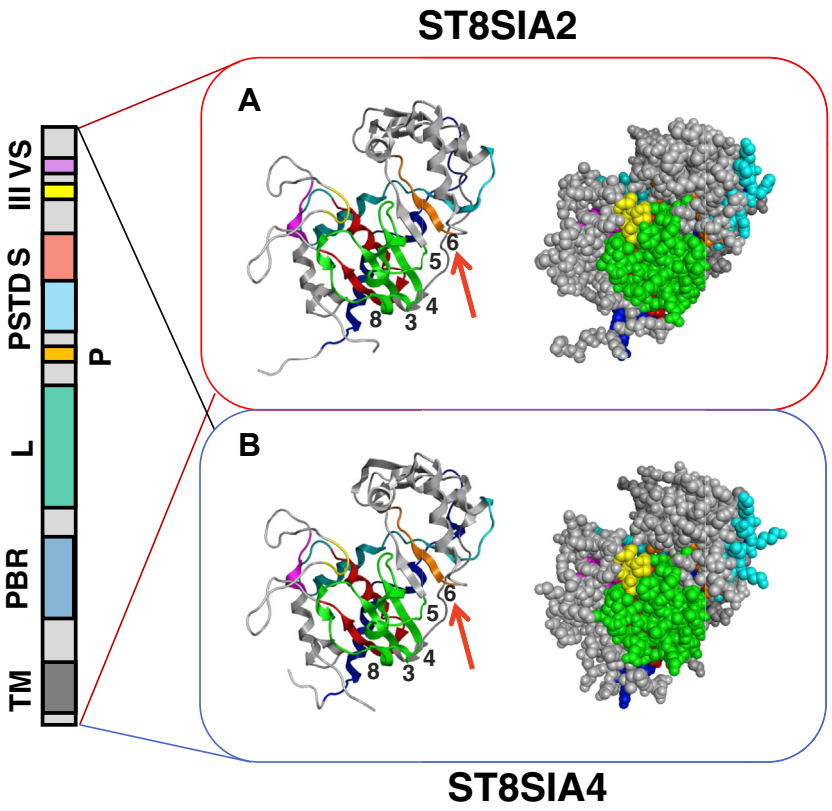

Figure 7. Ribbon and space-filling models of ST8SIA2 and ST8SIA4. *A* and *B*, the structures of ST8SIA2 (*A*) (residues 81–375) and ST8SIA4 (*B*) (residues 66–359) were predicted by Alphafold2. The schematic structures of the motifs and regions are colored. PBR (*blue*), sialyl motifs L (*green*), S (*red*), III (*yellow*), VS (*pink*), PSTD (*light blue*), and P motif (*orange*). *Red arrow* indicates the catalytic site. PBR, the polybasic region; PSTD, polysialyltransferase domain.

Based on the molecular modeling of ST8SIA2 and ST8SIA4 by AlphaFold2, five β-strands, consisting of the eighth β-strand in the sialyl motif S, the third and fourth ones in the sialyl motif L, fifth one β-strand right after the sialyl motif L, and the sixth one in the P motif, are aligned side-by-side and appear to form a large parallel β-sheet-like structure (Fig. 7). This parallel β-sheet-like structure appears to be important, because these five β-strands are highly pathogenic according to the InMeRF prediction (Fig. S2). It should be noted that the sixth β-strand (P motif) is buried inside the molecule. It cannot be seen from the outside at any directions, different from other four β-strands (Figs. 7 and S3), and is situated at the underneath of the active pocket of sialyl motif L and PSTD (Fig. 7). Usually, the surface of the molecule or the binding pocket is considered to be the most crucial region for the enzyme activity. In this regard, of known motifs in polySTs, the P motif is the first essential motif that is situated at the buried region. Since a series of the point-mutated enzymes in the P motif were properly expressed and correctly localized except for the P241A ST8SIA2 mutant (Figs. 2–4), the mutations in the P motif might keep overall structures of the mutants normal. In addition, molecular modeling of mutated P motifs in which each AA residue was replaced by not only Ala but also other hydrophobic AAs showed that the side chains of any AAs examined did not induce any structural changes, although the mutations of P241 in ST8SIA2 and P226 in ST8SIA4 slightly affected the length of the β-strand (Figs. S5 and S6). In contrast, most of them decreased or lost their enzyme activities. It is interesting to note that the enzyme activities (Figs. 2 and 3) were highly correlated to the energy calculation (Fig. 5), thus indicating that the calculated value is, as a whole, helpful to understand the relationship between impaired activity or pathogenicity and protein conformation. However, it should be noted that the proline mutant, P241A ST8SIA2, was clearly degraded (Fig. 2*A*), while the corresponding proline mutant, P226A ST8SIA4, was normally expressed (Fig. 3*A*). The large difference in the protein expression of these proline mutants could not be predicted either by the InMeRF program or the mutation energy calculation, because both prediction tools gave the same results between P241A ST8SIA2 and P226A ST8SIA4 (Figs. S1 and S5). We further analyzed the P241V/I/L ST8SIA2 and P226V/I/L mutations ST8SIA4 for the polySia and enzyme expression and found that all mutations other than P241A and P226A mutations showed the predicted results (Fig. S7). Therefore, we do not know why P/A mutations showed the different results. Other analysis is required to understand the cause.

The quality and quantity of polySia structure are important for the normal function of polySia and impairments of the regulated expression of polySia are considered to lead to the diseases such as mental disorder and cancer (3). The gene expression or the enzyme activity of ST8SIA2 and ST8SIA4 are important factors to regulate the quantity and quality of polySia. Therefore, the pathogenic region (P motif) other than

sialyl motifs that were also shown to be pathogenic might be key to understand the specific function of ST8SIA2 and 4 that are related to diseases. Another noteworthy finding by InMeRF was that ST3GAL3 (Fig. S3*A*) and ST6GAL2 (Fig. S3*B*) are predicted to be diseases-related genes. ST3GAL3, an ST3 β-galactoside α2,3-sialyltransferase 3, is a gene on chromosome 1p34, whose mutation A320P is known to associated with developmental and epileptic encephalopathy 15 (34). The mutation resides in the highly conserved sialyl motif S which is crucial for the binding of both donor and acceptor substrates. *In vitro* expression studies showed that this mutant reduced the secretion rate to 25% of control levels with no detectable enzyme activity. The InMeRF prediction (Fig. S1) shows that sialyl motif S (AAs 300–322) and other regions, including the stem region (AAs 29–159), are extensively pathogenic. ST6GAL2, an ST6 β-galactoside α2,6-sialyltransferase 2, has been shown to be involved in cancer (35), and any mutations in the region between sialyl motifs L and S are predicted to be pathogenic by InMeRF. This region does not have any known function so far, thus suggesting some novel roles.

PolySia expression is regulated by the gene expression and enzyme activity of polySTs. Almost all the P motif mutants tested in this study showed low activities and produced the dramatically small amount of polySia, although the expression levels of the enzymes were the same as that of WT except P241A ST8SIA2 (Figs. 2 and 3). These data suggest that the P motif regulates the enzyme properties rather than the protein expression. In addition, its regulation appears to be so precise and fine-tuned that subtle alterations in the P motif easily result in impairment of the enzyme properties. Interestingly, the polySia-NCAM synthesized by the P motif mutants of ST8SIA2 from S237A to F244A were lower in amount as well as smaller in size than that by the WT (Figs. 2*B* and S8). The same differences were observed between the polySia-NCAM synthesized by the P motif mutants of ST8SIA4 from W223A to F228A and that by the WT (Figs. 3*B* and S8). In the steric structure of ST8SIA2 and ST8SIA4 (Fig. 7), the P motif is situated close to the PSTD which is known to control the DP of polySia, and its structural changes may eventually affect the DP or the size of polySia-NCAM. PolySia can DP-dependently bind the brain-derived neurotrophic factor and the fibroblast growth factor 2, whose impairments are both involved in mental disorders and other diseases (3, 10). The P motif may thus be related to mental disorders through affecting the interaction of polySia with brain-derived neurotrophic factor and fibroblast growth factor 2. Based on the structural similarities and the pathogenicity of AA residues (Fig. S1), the P motif is also suggested to occur in ST8SIA1 and ST8SIA3, ST6GAL2, and ST3GAL1-5 as potential β-strand. Although these STs have no PSTD, the InMeRF predicts that their PSTD-corresponding regions are also highly pathogenic (Fig. S1). Therefore, in these STs, interaction between the P motif and the PSTD-corresponding region might play some role in fine-tuning of sialylation. The PBR region in ST8SIA2 and ST8SIA4 is involved in NCAM-specific polysialylation through binding to the acidic patch in NCAM. Since the P motif is very close to an α-helix at the end of the PBR, it may affect the conformation of PBR, and its impairments may possibly reduce polysialylation of NCAM, consistent with the reduced NCAM polysialylation in the P motif mutants (Figs. 2 and 3). This consideration is also relevant to the InMeRF's prediction that the PBR is also pathogenic. Interestingly, the InMeRF predicts that the PBR-corresponding region in ST8SIA1 is also highly pathogenic, although it has no acidic patch there. In ST8SIA1, the P motif may affect its interaction with the PBR-corresponding region to control the substrate species.

Experimental procedures

Materials

DNA polymerase KOD Plus Neo was purchased from Toyobo. The enhanced chemiluminescence Western blotting detection reagent (ECL) was purchased from ATTO. Bovine serum albumin (BSA) was purchased from Sigma-Aldrich. Polyvinylidene difluoride membranes were purchased from Millipore. Plasmids and *Dpn* I were purchased from Takara Bio. The PEI "Max" transfection reagent was purchased from Cosmobio. Alexa Fluor 555-labeled anti-chicken IgY, Alexa Fluor 488-labeled anti-rabbit IgG, and Nunc Multisorp surface immunoplates (#467340) were purchased from Thermo Fisher Scientific. The anti-polySia mouse monoclonal IgM antibody 12E3, which recognizes the oligo/polyNeu5Ac structure (DP ≥ 5), was provided by Dr Tatsunori Seki (Tokyo Medical University). The 735 monoclonal IgG antibodies that recognize the polyNeu5Ac structure (DP ≥ 11) were purified as described previously (36). Horseradish peroxidase (HRP)-conjugated anti-mouse IgG and IgM antibodies were purchased from American Qualex. Anti-His mouse monoclonal antibody (#66005-1-Ig) was purchased from Proteintech and Anti-V5 chicken polyclonal antibody (#A190-118A) was purchased from Funakoshi. Anti-TGN46 rabbit monoclonal antibody (#ab16059) was purchased from Abcam. Anti HSC70 mouse monoclonal antibody (#sc-7298) was purchased from Santa Cruz Biotechnology. HRP anti-human IgG (H+L) (#109-035-088) were purchased from Jackson Immunoresearch. PNGaseF was purchased from New England BioLabs.

Pathogenicity prediction of nonsynonymous single-nucleotide variants in InMeRF

The effects of AA substitutions were predicted using InMeRF (https://www.med.nagoya-u.ac.jp/neurogenetics/InMeRF/index.html). This algorithm predicts the pathogenicity of nonsynonymous single-nucleotide variants using 150 discriminant models independently generated for all possible AA substitutions. The analysis was performed using genome assembly version GRCh37/hg19. We predicted the pathogenicity in human sialyltransferase genes; gene name (Ensembl ID): ST3GAL1 (ENSP00000414073), ST3GAL2 (ENSP00000377257), ST3GAL3 (ENSP00000317192), ST3GAL4 (ENSP00000394354), ST3GAL5 (ENSP00000491316), ST3GAL6 (ENSP00000417376), ST6GAL1 (ENSP00000169298), ST6GAL2 (ENSP00000386942), ST6GALNAC1 (ENSP00000156626), ST6GALNAC2 (ENSP00000225276),

ST6GALNAC3 (ENSP00000329214), ST6GALNAC4 (ENSP00000336733), ST6GALNAC5 (ENSP00000417583), ST6GALNAC6 (ENSP00000362239), ST8SIA1 (ENSP00000379353), ST8SIA2 (ENSP00000268164), ST8SIA3 (ENSP00000320431), ST8SIA4 (ENSP00000231461), ST8SIA5 (ENSP00000321343), and ST8SIA6 (ENSP00000366827). We calculated pathogenicity rates (%) (=100 × [number of AA substitutions predicted to be pathogenic in InMeRF]/[number of all possible AA substitutions]).

Comparative sequence analysis

Human ST8SIA2 and ST8SIA4 sequences were obtained from the National Center for Biotechnology Information gene database (https://www.ncbi.nlm.nih.gov/gene/). All sequences were aligned using GENETYX ver.13.

Construction of the plasmids and establishment of cells

Human ST8SIA2 and ST8SIA4 cDNA were cloned into a pBApo-EF1α vector (Takara Bio) containing a C-terminal V5 epitope tag and a stop codon before the His6 tag. The resulting plasmids containing the DNA sequences for ST8SIA2 or ST8SIA4 served as templates for the creation of all the P motif mutants, in which each residue within the P motif was replaced with alanine. All mutants were created using KOD-plus-Neo and *Dpn* I according to the manufacturer's instructions, using the oligonucleotide primers listed in Table 1. To confirm the presence of the mutations, the resultant DNA was sequenced using DNA sequencing at Eurofins Genomics in Tokyo.

Mouse neuroblastoma Neuro2A cells (2 × 10^5 cells) were seeded in a six-well plate and cultured for 24 h. The cells on each plate were then transfected with 3 μg of each plasmid in 200 μl phosphate-buffered saline (PBS) containing 6 μg PEI Max. The cells were incubated with the transfection mixture for 4 h at 37 °C, followed by the addition of 2 ml Dulbecco's Modified Eagle Medium containing 10% fetal bovine serum (FBS). After 48 h, the cells were homogenized in a lysis buffer (1% Triton-X100, 1 mM phenylmethanesulfonyl fluoride, protease inhibitors: 1 μg/ml aprotinin, 1 μg/ml leupeptin, 1 μg/ml pepstatin, 2 μg/ml antipain, 10 μg/ml benzamidine, 1 mM EDTA, 50 mM NaF, 10 mM β-glycerophosphate, 10 mM sodium pyrophosphate, and 1 mM sodium o-vanadate in PBS). Homogenates were incubated on ice for 1 h and centrifuged at 10,000 rpm for 15 min at 4 °C. The supernatant was collected, and protein concentrations were determined using the bicinchoninic acid assay.

Western blotting

To remove *N*-glycans, some of the cell lysates for detection with the anti-His antibody were incubated in 1× Glycoprotein Denaturing Buffer (New England Biolabs) at 100 °C for 10 min. The de-*N*-glycosylation reaction mixtures contained 1× Glycobuffer2 (New England Biolabs), 1% NP-40, and 20 U PNGaseF, and were incubated at 37 °C overnight. All samples were dissolved in Laemmli buffer containing 5% mercaptoethanol and were subsequently incubated at 60 °C for 20 min for detection with the anti-polySia antibodies, 12E3 and 735, or at 100 °C for 3 min for detection with the anti-His antibody. Proteins from each sample (10 μg as BSA) were separated by 7.5% SDS-PAGE and blotted onto polyvinylidene difluoride membranes. The membrane was then blocked with phosphate-buffered saline with 0.1% Tween 20 Detergent (PBST) at 25 °C for 1 h containing 1% BSA for the anti-glycan antibody or 1% skim milk for the anti-protein antibody. The membrane was incubated with primary antibodies, the 12E3 IgM antibody (37), the 735 monoclonal IgG antibody (38), the anti-His monoclonal IgG_1 antibody (1:1000), and the anti-HSC70 monoclonal IgG_{2a} antibody (1:1000) at 4 °C overnight. After washing with PBST, the membrane was incubated with a secondary antibody, HRP-conjugated anti-mouse IgG + M (0.2 μg/ml), or HRP-conjugated anti-human IgG (0.08 μg/ml) at 37 °C for 1 h. After washing with PBST, the immunoblots were developed using an enhanced chemiluminescence (ECL) western blotting detection reagent.

Table 1
Primers used to create polyST mutant

Primer set	Mutant	Template	Primer sequence
1	S236A	ST8SIA2	5′-cacagcctcaatggcgcaatcctgtggatccctgccttc-3′ 5′-gccattgaggctgtgcagccgttgcagcagcttc-3′
2	I237A	ST8SIA2	5′-agcctcaatggcagcgcactgtggatccctgccttc-3′ 5′-gctgccattgaggctgtgcagccgttgcagcag-3′
3	L238A	ST8SIA2	5′-ctcaatggcagcatcgcatggatccctgccttcatg-3′ 5′-gatgctgccattgaggctgtgcagccgttgcag-3′
4	W239A	ST8SIA2	5′-aatggcagcatcctggcaatccctgccttcatggcc-3′ 5′-caggatgctgccattgaggctgtgcagccgttgc-3′
5	I240A	ST8SIA2	5′-ggcagcatcctgtgggctcctgccttcatggcccgg-3′ 5′-ccacaggatgctgccattgaggctgtgcagccg-3′
6	P241A	ST8SIA2	5′-agcatcctgtggatcgctgccttcatggcccggggc-3′ 5′-gatccacaggatgctgccattgaggctgtgcag-3′
7	F243A	ST8SIA2	5′-ctgtggatccctgccgctatggcccggggcggcaag-3′ 5′-ggcagggatccacaggatgctgccattgaggctg-3′
8	M244A	ST8SIA2	5′-tggatccctgccttcgctgcccggggcggcaaggag-3′ 5′-gaaggcagggatccacaggatgctgccattgag-3′
9	R246A	ST8SIA2	5′-cctgccttcatggccgcaggcggcaaggagcgtgttg-3′ 5′-ggccatgaaggcagggatccacaggatgctgcc-3′
10	S221A	ST8SIA4	5′-tccatgctgaatgacgctgtcctttggattcctgctttc-3′ 5′-gtcattcagcatggaaagtctatgcacaaatttttc-3′
11	V222A	ST8SIA4	5′-atgctgaatgacagtgcactttggattcctgctttc-3′ 5′-actgtcattcagcatggaaagtctatgcacaaatttttc-3′
12	L223A	ST8SIA4	5′-ctgaatgacagtgtcgcttggattcctgctttcatg-3′ 5′-gacactgtcattcagcatggaaagtctatgcac-3′
13	W224A	ST8SIA4	5′-aatgacagtgtccttgcaattcctgctttcatggtc-3′ 5′-aaggacactgtcattcagcatggaaagtctatg-3′
14	I225A	ST8SIA4	5′-gacagtgtcctttgggctcctgctttcatggtcaaagg-3′ 5′-ccaaaggacactgtcattcagcatggaaagtc-3′
15	P226A	ST8SIA4	5′-agtgtcctttggattgctgctttcatggtcaaaggag-3′ 5′-aatccaaaggacactgtcattcagcatggaaag-3′
16	F228A	ST8SIA4	5′-ctttggattcctgctgccatggtcaaaggaggagag-3′ 5′-agcaggaatccaaaggacactgtcattcagcatgg-3′
17	M229A	ST8SIA4	5′-tggattcctgctttcgcggtcaaaggaggagagaag-3′ 5′-gaaagcaggaatccaaaggacactgtcattcag-3′
18	V230A	ST8SIA4	5′-attcctgctttcatggccaaaggaggagagaagcacg-3′ 5′-catgaaagcaggaatccaaaggacactgtcattc-3′
19	K231A	ST8SIA4	5′-cctgctttcatggtcgccggaggagagaagcacgtgg-3′ 5′-gaccatgaaagcaggaatccaaaggacactgtc-3′

Cell staining

Neuro2A cells (2 × 10^5 cells) were seeded in six-well plates on coverslips and grown in a 5% CO_2 incubator at 37 °C. The cells in each plate were transfected as described above. Cells were incubated with the transfection mixture for 4 h at 37 °C,

followed by the addition of 2 ml Dulbecco's Modified Eagle Medium containing 10% FBS. After 24 h, the cells were washed with PBS and fixed with 4% paraformaldehyde at room temperature for 8 min. After washing, the cells were permeabilized with 0.1% TritonX-100 in PBS at room temperature for 15 min. The permeabilized cells were blocked with PBS containing 2% BSA for 1 h and then incubated with the following primary antibodies diluted in blocking buffer for 1 h at room temperature: anti-V5 tag antibody (1:200) to detect the expression and localization of ST8SIA6, ST8SIA6 swapping mutants, ST8SIA2 and ST8SIA4, and the anti-TGN46 antibody (1:200) to detect *trans*-Golgi apparatus (19). After washing with PBS, the cells were incubated for 30 min with the following secondary antibodies diluted in blocking buffer: AlexaFluoro555-labeled anti-chicken IgY (1:1000) to visualize protein localization and Alexa Fluoro488-labeled anti-rabbit IgG (1:500) to visualize the localization marker. After washing with PBS, the cells were incubated with 1 μg/ml DAPI (4′,6-diamidino-2-phenylindole) diluted in water for 15 min at 37 °C. After washing with water, the coverslips were mounted on glass slides using 20 μl Mowiol. The cells were observed under a confocal scanning fluorescence microscope (Olympus).

Bioinformatics analysis of ST8SIA2 and ST8SIA4

The structures of ST8SIA2 and ST8SIA4 were predicted using AlphaFold2 (30, 31).

Calculation of mutation energy

The AA sequence of human ST8SIA2 and ST8SIA4 was obtained from the Universal Protein Resource database (UniProt ID: Q92186 and Q92187). The 3D structural models of ST8SIA2 and ST8SIA4 were obtained from the AlphaFold2 Protein Structure Database (31), and a 3D model of each variant was prepared using the Calculate Mutation Energy/Stability module in Discovery Studio 2021 (BIOVIA, Dassault Systèmes). Mutation energy was calculated with the Calculate Mutation Energy/Stability module in Discovery Studio 2021 based on CHARMm (version 44.2) force field (39, 40).

Data analysis

All values are expressed as the mean ± SEM.

Data availability

All data are contained within the manuscript.

Supporting information—This article contains supporting information.

Acknowledgments—We thank Prof. Kinji Ohno (Nagoya University, School of Medicine) for helpful discussions about InMeRF program. We also thank Ayane Naramura for technical contribution. R. H. was supported by Nagoya University CIBoG WISE program from MEXT.

Author contributions—C. S. conceptualization; R. H., M. H., K. H., S. M., S. O., Y. Y., D. W., K. K., and C. S. methodology; R. H., M. H., K. H., S. M., S. O., Y. Y., D. W., K. K., and C. S. investigation; R. H., M. H., K. H., S. M., S. O., Y. Y., D. W., K. K., and C. S. formal analysis. R. H., Y. Y., and C. S. writing–original draft; R. H., Y. Y., K. K., and C. S. writing–review and editing.

Funding and additional information—This research was funded by Japan Agency for Medical Research and Development grant number [18ae0101069h0003; 19ae0101069h0004; 20ae0101069h0005; 20gm6410007h0001, 21gm6410007h0002, 22gm6410007h0003] (to C. S.) and a Grant-in-Aid for Scientific Research (B) (21H02425) from JSPS (to C. S.). A part of this research was also funded by "Nagoya University Interdisciplinary Frontier Fellowship" supported by Nagoya University and JST, the establishment of university fellowships toward the creation of science technology innovation, Grant Number JPMJFS2120 and 23KJ1063 from JSPS (to R. H.).

Conflict of interest—The authors declare that they have no conflicts of interest with the contents of this article.

Abbreviations—The abbreviations used are: CMP-Sia, cytidine 5′-monophospho-sialic acid; DP, degree of polymerization; InMeRF, Individual Meta Random Forest program; NCAM, neural cell adhesion molecule; PBR, polybasic region; P motif, Pathogenic motif; polySia, polysialic acid; PSTD, polysialyltransferase domain; Sia, sialic acid; ST, sialyltransferase; WT, wildtype.

References

1. Schauer, R., and Kamerling, J. P. (2018) Exploration of the sialic acid world. *Adv. Carbohydr. Chem. Biochem.* **75**, 1–213
2. Harduin-Lepers, A. (2023) The vertebrate sialylation machinery: structure-function and molecular evolution of GT-29 sialyltransferases. *Glycoconj. J.* **40**, 473–492
3. Sato, C., and Kitajima, K. (2021) Polysialylation and disease. *Mol. Aspects Med.* **79**, 100892
4. Bonfanti, L. (2006) PSA-NCAM in mammalian structural plasticity and neurogenesis. *Prog. Neurobiol.* **80**, 129–164
5. Johnson, C. P., Fujimoto, I., Rutishauser, U., and Leckband, D. E. (2005) Direct evidence that neural cell adhesion molecule (NCAM) polysialylation increases intermembrane repulsion and abrogates adhesion. *J. Biol. Chem.* **280**, 137–145
6. Kanato, Y., Kitajima, K., and Sato, C. (2008) Direct binding of polysialic acid to a brain-derived neurotrophic factor depends on the degree of polymerization. *Glycobiology* **18**, 1044–1053
7. Ono, S., Hane, M., Kitajima, K., and Sato, C. (2012) Novel regulation of fibroblast growth factor 2 (FGF2)-mediated cell growth by polysialic acid. *J. Biol. Chem.* **287**, 3710–3722
8. Sato, C., and Kitajima, K. (2019) Sialic acids in neurology. *Adv. Carbohydr. Chem. Biochem.* **76**, 1–64
9. Takashima, S. (2008) Characterization of mouse sialyltransferase genes: their evolution and diversity. *Biosci. Biotechnol. Biochem.* **72**, 1155–1167
10. Sato, C., and Kitajima, K. (2013) Disialic, oligosialic and polysialic acids: distribution, functions and related disease. *J. Biochem.* **154**, 115–136
11. Sasaki, K., Kurata, K., Kojima, N., Kurosawa, N., Ohta, S., Hanai, N., *et al.* (1994) Expression cloning of a GM3-specific alpha-2,8-sialyltransferase (GD3 synthase). *J. Biol. Chem.* **269**, 15950–15956
12. Kono, M., Yoshida, Y., Kojima, N., and Tsuji, S. (1996) Molecular cloning and expression of a fifth type of alpha2,8-sialyltransferase (ST8Sia V). Its substrate specificity is similar to that of SAT-V/III, which synthesize GD1c, GT1a, GQ1b and GT3. *J. Biol. Chem.* **271**, 29366–29371
13. Volkers, G., Worrall, L. J., Kwan, D. H., Yu, C. C., Baumann, L., Lameignere, E., *et al.* (2015) Structure of human ST8SiaIII sialyltransferase provides insight into cell-surface polysialylation. *Nat. Struct. Mol. Biol.* **22**, 627–635

14. Yoshida, Y., Kojima, N., Kurosawa, N., Hamamoto, T., and Tsuji, S. (1995) Molecular cloning of Sia alpha 2,3Gal beta 1,4GlcNAc alpha 2,8-sialyltransferase from mouse brain. *J. Biol. Chem.* **270**, 14628–14633
15. Takashima, S., Ishida, H. K., Inazu, T., Ando, T., Ishida, H., Kiso, M., *et al.* (2002) Molecular cloning and expression of a sixth type of alpha 2,8-sialyltransferase (ST8Sia VI) that sialylates O-glycans. *J. Biol. Chem.* **277**, 24030–24038
16. Kojima, N., Yoshida, Y., Kurosawa, N., Lee, Y., and Tsuji, S. (1995) Enzymatic activity of a developmentally regulated member of the sialyltransferase family (STX): evidence for alpha 2,8-sialyltransferase activity toward N-linked oligosaccharides. *FEBS Lett.* **360**, 1–4
17. Scheidegger, E., Lackie, P., Papay, J., and Roth, J. (1994) *In vitro* and *in vivo* growth of clonal sublines of human small cell lung carcinoma is modulated by polysialic acid of the neural cell adhesion molecule. *Lab. Invest.* **70**, 95–106
18. Eckhardt, M., Mühlenhoff, M., Bethe, A., Koopman, J., Frosch, M., and Gerardy-Schahn, R. (1995) Molecular characterization of eukaryotic polysialyltransferase-1. *Nature* **373**, 715–718
19. Hatanaka, R., Araki, E., Hane, M., Go, S., Wu, D., Kitajima, K., *et al.* (2022) The α2,8-sialyltransferase 6 (St8sia6) localizes in the ER and enhances the anchorage-independent cell growth in cancer. *Biochem. Biophys. Res. Commun.* **608**, 52–58
20. Colley, K. J., Kitajima, K., and Sato, C. (2014) Polysialic acid: biosynthesis, novel functions and applications. *Crit. Rev. Biochem. Mol. Biol.* **49**, 498–532
21. Rollenhagen, M., Kuckuck, S., Ulm, C., Hartmann, M., Galuska, S. P., Geyer, R., *et al.* (2012) Polysialylation of the synaptic cell adhesion molecule 1 (SynCAM 1) depends exclusively on the polysialyltransferase ST8SiaII in vivo. *J. Biol. Chem.* **287**, 35170–35180
22. Galuska, S. P., Rollenhagen, M., Kaup, M., Eggers, K., Oltmann-Norden, I., Schiff, M., *et al.* (2010) Synaptic cell adhesion molecule SynCAM 1 is a target for polysialylation in postnatal mouse brain. *Proc. Natl. Acad. Sci. U. S. A.* **107**, 10250–10255
23. Stamatos, N. M., Zhang, L., Jokilammi, A., Finne, J., Chen, W. H., El-Maarouf, A., *et al.* (2014) Changes in polysialic acid expression on myeloid cells during differentiation and recruitment to sites of inflammation: role in phagocytosis. *Glycobiology* **24**, 864–879
24. Bhide, G. P., Fernandes, N. R., and Colley, K. J. (2016) Sequence requirements for neuropilin-2 recognition by ST8SiaIV and polysialylation of its O-glycans. *J. Biol. Chem.* **291**, 9444–9457
25. Kojima, N., Tachida, Y., Yoshida, Y., and Tsuji, S. (1996) Characterization of mouse ST8Sia II (STX) as a neural cell adhesion molecule-specific polysialic acid synthase. Requirement of core alpha1,6-linked fucose and a polypeptide chain for polysialylation. *J. Biol. Chem.* **271**, 19457–19463
26. Galuska, S., Geyer, H., Bleckmann, C., Röhrich, R., Maass, K., Bergfeld, A., *et al.* (2010) Mass spectrometric fragmentation analysis of oligosialic and polysialic acids. *Anal. Chem.* **82**, 2059–2066
27. Cremer, H., Lange, R., Christoph, A., Plomann, M., Vopper, G., Roes, J., *et al.* (1994) Inactivation of the N-CAM gene in mice results in size reduction of the olfactory bulb and deficits in spatial learning. *Nature* **367**, 455–459
28. Takeda, J. I., Nanatsue, K., Yamagishi, R., Ito, M., Haga, N., Hirata, H., *et al.* (2020) InMeRF: prediction of pathogenicity of missense variants by individual modeling for each amino acid substitution. *NAR Genom. Bioinform.* **2**, lqaa038
29. Foley, D., Swartzentruber, K., and Colley, K. (2009) Identification of sequences in the polysialyltransferases ST8Sia II and ST8Sia IV that are required for the protein-specific polysialylation of the neural cell adhesion molecule, NCAM. *J. Biol. Chem.* **284**, 15505–15516
30. Varadi, M., Anyango, S., Deshpande, M., Nair, S., Natassia, C., Yordanova, G., *et al.* (2022) AlphaFold Protein Structure Database: massively expanding the structural coverage of protein-sequence space with high-accuracy models. *Nucleic Acids Res.* **50**, D439–D444
31. Jumper, J., Evans, R., Pritzel, A., Green, T., Figurnov, M., Ronneberger, O., *et al.* (2021) Highly accurate protein structure prediction with AlphaFold. *Nature* **596**, 583–589
32. Datta, A. K., and Paulson, J. C. (1995) The sialyltransferase "sialylmotif" participates in binding the donor substrate CMP-NeuAc. *J. Biol. Chem.* **270**, 1497–1500
33. Datta, A. K., Sinha, A., and Paulson, J. C. (1998) Mutation of the sialyltransferase S-sialylmotif alters the kinetics of the donor and acceptor substrates. *J. Biol. Chem.* **273**, 9608–9614
34. Edvardson, S., Baumann, A. M., Mühlenhoff, M., Stephan, O., Kuss, A. W., Shaag, A., *et al.* (2013) West syndrome caused by ST3Gal-III deficiency. *Epilepsia* **54**, e24–e27
35. Cheng, J., Wang, R., Zhong, G., Chen, X., Cheng, Y., Li, W., *et al.* (2020) ST6GAL2 downregulation inhibits cell adhesion and invasion and is associated with improved patient survival in breast cancer. *Onco Targets Ther.* **13**, 903–914
36. Sato, C., Fukuoka, H., Ohta, K., Matsuda, T., Koshino, R., Kobayashi, K., *et al.* (2000) Frequent occurrence of pre-existing alpha 2 -> 8-linked disialic and oligosialic acids with chain lengths up to 7 Sia residues in mammalian brain glycoproteins - prevalence revealed by highly sensitive chemical methods and anti-di-, oligo-, and poly-Sia antibodies specific for defined chain lengths. *J. Biol. Chem.* **275**, 15422–15431
37. Inoko, E., Nishiura, Y., Tanaka, H., Takahashi, T., Furukawa, K., Kitajima, K., *et al.* (2010) Developmental stage-dependent expression of an alpha2, 8-trisialic acid unit on glycoproteins in mouse brain. *Glycobiology* **20**, 916–928
38. Hayakawa, K., Hane, M., Hamagami, H., Imai, M., Tanaka, H., Kitajima, K., *et al.* (2023) Interactions between polysialic acid and dopamine-lead compounds as revealed by biochemical and in silico docking simulation analyses. *Glycoconj J.* **40**, 461–471
39. Brooks, B. R., Bruccoleri, R. E., Olafson, B. D., States, D. J., Swaminathan, S., Karplus, M., *et al.* (1983) CHARMM: a program formacromolecular energy, minimization, and dynamics calculations. *J. Comput. Chem.* **4**, 187–217
40. Brooks, B. R., Brooks, C. L., Mackerell, A. D., Nilsson, L., Petrella, R. J., Roux, B., *et al.* (2009) CHARMM: the biomolecular simulation program. *J. Comput. Chem.* **30**, 1545–1614